

## Investigation the Performance of Stream Water Wheel Turbines using CFD Techniques

Mohammad A. AL-DABBAGH  
Northern Technical University

**Abstract:** A stream water wheel is a machine for converting the energy of moving water into power. It consists of a large metal wheel, with a number blades arranged on the outer rim which allows the wheel to be rotated by the water striking the blades. Water wheels were used since ancient as a primary source of power. It was used for irrigation, grain milling and supplying villages with water. In the present study, a stream water wheel turbine of 5 m in diameter is numerically simulated using ANSYS-CFX package under different flow conditions. The wake region behind the turbine is monitored where it influences on other turbines next to it. The simulation results have shown that in case of constructing a farm of wheel turbines, the streamwise span should not be less than 6 m. The stream wheel turbines works normally at a tip speed ratio TSR less than unity.

**Keywords:** Hydrokinetic turbines, Stream-water wheel turbine, Efficiency, CFD

### Introduction

The water wheel was used as a primary source of power since ancient times (Denny 2004). It has been used for irrigation, grain milling and supplying villages with drinking water. It was considered as the first method that is used to replace the muscular effort of the humans and animals to perform a mechanical energy. The oldest water wheel, which is in a reserved panel of a mosaic is dating back to 4000 years BC, was built in Damascus (Institute of Technology – Baghdad – Iraq 2013) and another ancient one was found in Hama (Figure 1). The water power was used also in Mesopotamia and by Egyptians. They are harnessing energy from flux water by waterwheels giving revolving energy for different purposes (Schlager and Weisblatt 2006; Muller et al. 2007). Ancient Greeks, Chinese and Romans have also constructed great waterwheels to grind their grains. The Roman Architect Vitruvius already mentioned the stream wheels (Muller et al. 2007). At the end of the 18th century, about 500,000 watermills were working in Europe (Quaschnig 2010).



Figure 1. The water wheel that exists in Hama

Water wheels are categorized by the method that make water entering the turbine, relative to the wheel's axle (Figure 2). The overshot & pitch back water wheels are appropriate where there is water level difference of no more than 2 meters, often in connotation with a small basin. Breastshot and undershot wheels can be utilized with streams or high volume currents with big lakes (Paudel et al. 2013).

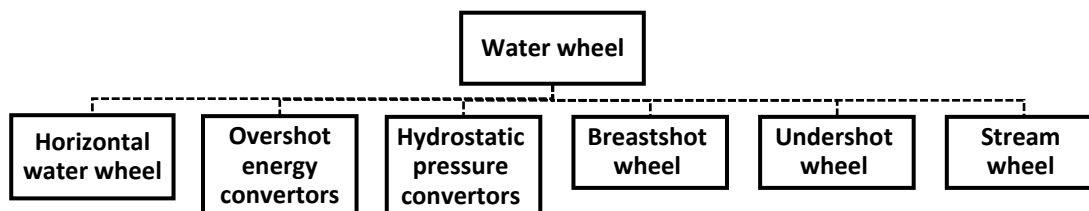


Figure 2. Water wheel classification

Many investigations have shown that water wheels are theoretically and economically promising choices for low head places with an efficiency range of 75-85% over changeable flow currents. Using a water wheel with big size chambers and low angular speeds aquatic life out of danger and the geometrical shape of the wheel provide well sediment passage and make it easier to floating the rubbish (Muller and Kauppert 2004). In addition, a strong and easy design of a water wheel leads to fewer works in constructing, working and repairing the structure, which result in less primary operation and maintenance prices (Woods et al. 2010). Table 1 shows specifications of different water wheels.

Table 1. Technical specifications of some water wheel turbines

Turbine type	Classification	Dimension (m)	Rated power (kw)	No. of blades	Working head (m)	Flow rate m <sup>2</sup> /sec	Efficiency %
Horizontal water wheel		--	--	Multi	--	--	15-30
Overshot energy convertors	Overshot water wheel						
	Reversible water wheel	3-20	1.3-20	8-16	2.5-10	0.1-0.2	60-80
	Backshot water wheel						
Hydrostatic pressure convertors	Suspension water wheel						
	Back pres. Turbine Hydrostatic machine	0.8-5	2-12	Multi	1-2.5	0.5-0.6	60-90
Breastshot wheels	Hydrostatic pres. wheel						
	Sagebien wheel	4-8	5-200	Multi	0.75-5	0.35-0.65	50-75
Undershot wheel	Aqualienne wheel						
	Zuppinger wheel	2-4H	5-100	Multi	0.5 -3	0.5-0.95	35-76
Stream wheels	Poncelet wheel						
	Subcritical wheel	2-6	1.7-33	Multi	0.4-1.5	2.5-3.75	30-68
	Supercritical wheel						
	Deep water wheel						

### Numerical Model

In the present study, because that the domain includes a rotating object, the wheel, a complex flow regime is expected to be occurred. The Reynolds stress-omega transport turbulence model is dependent as the powerful tool for analyzing the flow around and behind the structure. The occurrence of flow separation is maintained by this model. In addition, the complicated regimes represented by swirling and rotating fluids are treated well by this model. Because that this model treats the boundary layer near wall and be efficient for low Reynolds numbers besides the high ones, it is suitable for investigating the flow behavior in shallow streams where water wheel turbines work (Speziale et al. 1991; Biscarini et al. 2010; Chevallet et al. 2012). The basic equations representing the Reynolds stress- omega turbulence model are given as follow:

$$\frac{\partial}{\partial t}(\rho \overline{u'_i u'_j}) + \frac{\partial}{\partial x_k}(\rho u_k \overline{u'_i u'_j}) = -\frac{\partial}{\partial x_k} \left[ \rho \overline{u'_i u'_j u'_k} + p'(\delta_{kj} u'_i + \delta_{ik} u'_j) \right] + \frac{\partial}{\partial x_k} \left[ \mu \frac{\partial}{\partial x_k} (\overline{u'_i u'_j}) \right] - \rho \left[ \overline{u'_i u'_k} \frac{\partial u_j}{\partial x_k} + \overline{u'_j u'_k} \frac{\partial u_i}{\partial x_k} \right] - \rho \beta (g_i \overline{u'_j \theta}) + p' \left( \frac{\partial u'_i}{\partial x_j} + \frac{\partial u'_j}{\partial x_i} \right) - 2\mu \frac{\partial u'_i}{\partial x_k} \frac{\partial u'_j}{\partial x_k} - 2\rho \Omega_k (\overline{u'_j u'_m} \varepsilon_{ikm} + \overline{u'_i u'_m} \varepsilon_{jkm}) + S_{user}$$

While the left side of the equation represents the summation of the local time derivative and the convection, the right side equals to the summation of molecular diffusion and pressure strain besides the user defined sources minus the turbulent diffusion, stress production, buoyancy production, dissipation and production by system rotation, respectively.

### Model Setup

The present study involves investigation the performance of stream water wheel turbines. Simulation analyses are conducted using CFD techniques under two different flow velocities of 1.0 m s<sup>-1</sup> and 2.0 m s<sup>-1</sup>. A wheel turbine with 12 blades is designed and placed at 5 m far from the inlet of a rectangular channel of 30 m length, 5 m height and 1 m width with a horizontal layout (Figure 3). The side walls are given a symmetry boundary condition and the bottom was smooth wall. The upper face of the domain is considered as free to atmosphere. The left face of the channel is considered as the channel entrance and given an inlet boundary condition while the right side, which is the channel outlet, was given a zero pressure. A clear water is used with a density of 998 kg m<sup>-3</sup> and flowing with no any sediments.

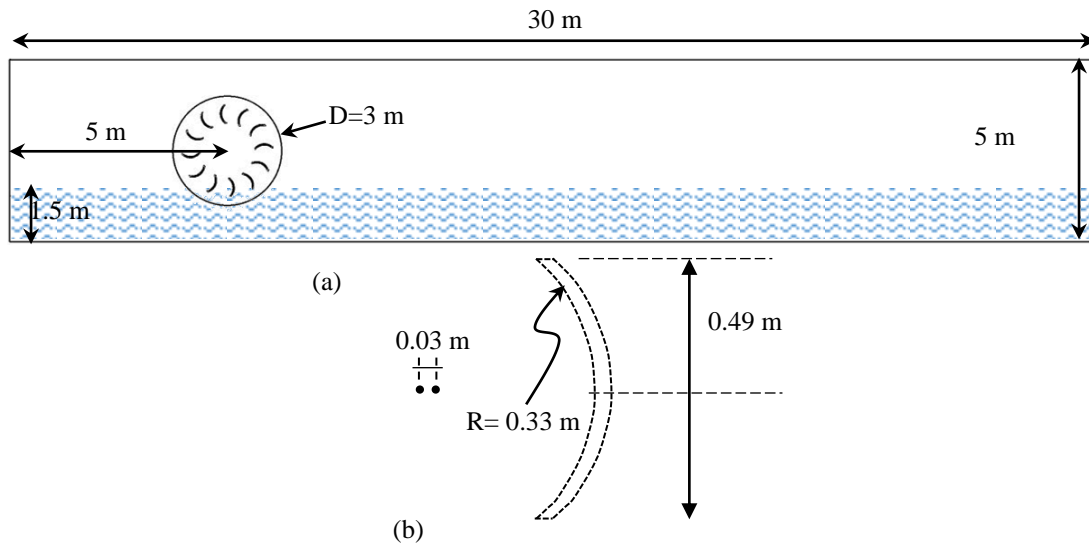


Figure 3. a. Channel domain and wheel position, b. blade's design

### Meshing Process

In computational fluid dynamics simulation, the solution progress is constraint by mesh type and the refinement rate. When mesh elements are coarse, bad quality, the controlled volume will be instable and the solution progress will be diverged or may reach the end of the solution with high errors. This is attributed to that the output results from an element are dependent as input for the next element, so, when the element is coarse, large volume, no data will be available for some interested points inside. Therefore, the output results will be unsatisfied. Nevertheless, fine elements increase the rate of convergence and the simulation analysis progresses smoothly with low error residuals. Many types of mesh are provided by ANSYS package, which are tetrahedron, hex, prism and quadrilateral shapes. Each type serves a specific region where it is not recommended to use hex meshing for swept bodies while tetrahedron elements are good for moving or rotating machines. In the present study, the domain includes rotating object, therefore, triangle elements are used. Figure 4 shows the initial mesh in compare with the final mesh at the end of the simulation. It shows how the mesh becomes finer at the regions close to the blades while in the middle, the elements are coarse. This is attributed to that the entire region is free of water except some amounts which are lifted by the blades.

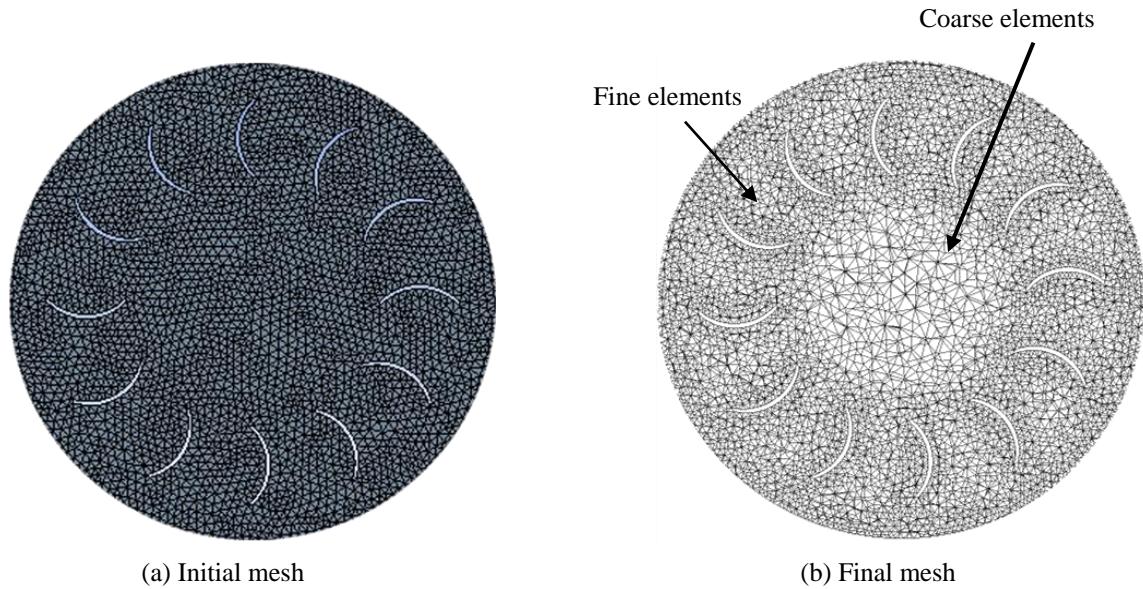


Figure 4. Initial and final mesh

## Simulation Results

This study performs simulation analyses in order to investigate the flow pattern downstream stream water wheel turbines under different flow conditions. A constant number of blades is taken, which are 12 blades. The performance of the turbine is evaluated at different tip speed ratios. The tip speed ratio (TSR) is defined as the ratio of the rotational velocity of a turbine to the velocity of the flowing fluid. The TSR is considered as an important parameter should be taken into account to specify the optimum range of the angular velocity that gives a highest power value. (Cao 2011; Winchester and Quayle 2011; Niblick 2012; Syed Shah et al. 2013).

$$\lambda = \frac{\omega R}{v_{\infty}} \quad (1)$$

Where:

$\lambda$ : tip speed ratio (TSR).

$\omega$ : angular speed of turbine.

R: turbine radius.

$v_{\infty}$ : free stream velocity.

The performance of the turbine is evaluated in terms of the power coefficient or the efficiency.

The turbine efficiency or the performance coefficient is a dimensionless parameter describing the performance of the turbine, which is determined as follow;

$$\eta = \frac{P_t}{P_w} = \frac{T\omega}{0.5\rho A v_{fluid}^3} \quad (2)$$

Where:

$P_t$ : turbine power.

$P_w$ : flowing water power.

T: torque developed by turbine shaft (N-m).

$\omega$ : angular velocity of the turbine ( $\text{rads}^{-1}$ ).

$\rho$ : water density ( $\text{kgm}^{-3}$ ).

A: turbine's frontal cross-sectional area ( $\text{m}^2$ ).

$v_{fluid}$ : water velocity ( $\text{m s}^{-1}$ ).

The simulation results have shown that performance of the wheel turbine under the two given velocities was the same. The water level raised up at the upstream side of the turbine due to flow resistance by the submerged body. For the given velocities, the flowing water downstream the turbine shows similar behavior. It is noticed that downstream the turbine at a distance of about 3 times the diameter of the wheel, the water level returns to

its initial case (Figures 5 and 6). The performance of the model is investigated at different tip speed ratios TSRs' where the turbine reached the maximum efficiency of about 0.15 at a TSR of about 0.42. At high TSR values, the turbine behaved similarly under the two given velocities where the efficiency was inversly proportional to the TSR values above 0.42 (Figure 7). Figure 8 shows the turbulence region at different velocities and rotational speeds in term of the water volume fraction.

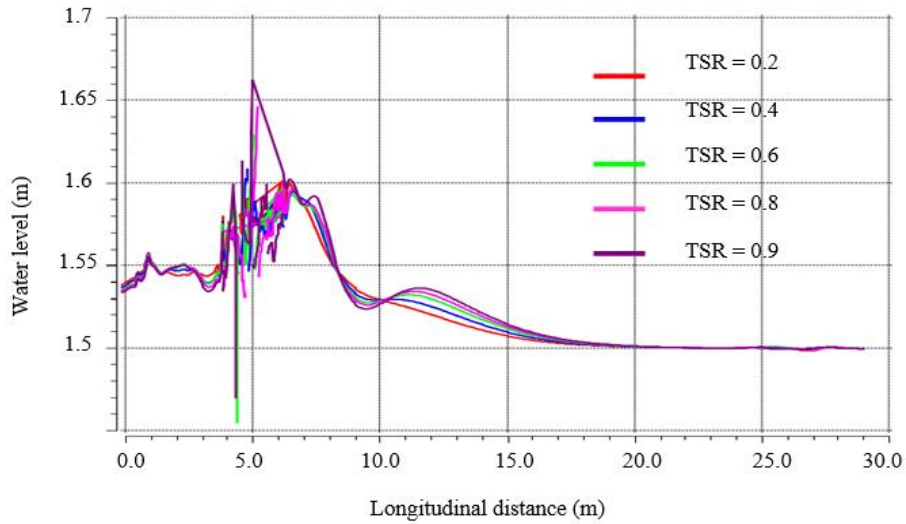


Figure 5. Water level at different distances along the channel at a flow velocity of  $1.0 \text{ m s}^{-1}$

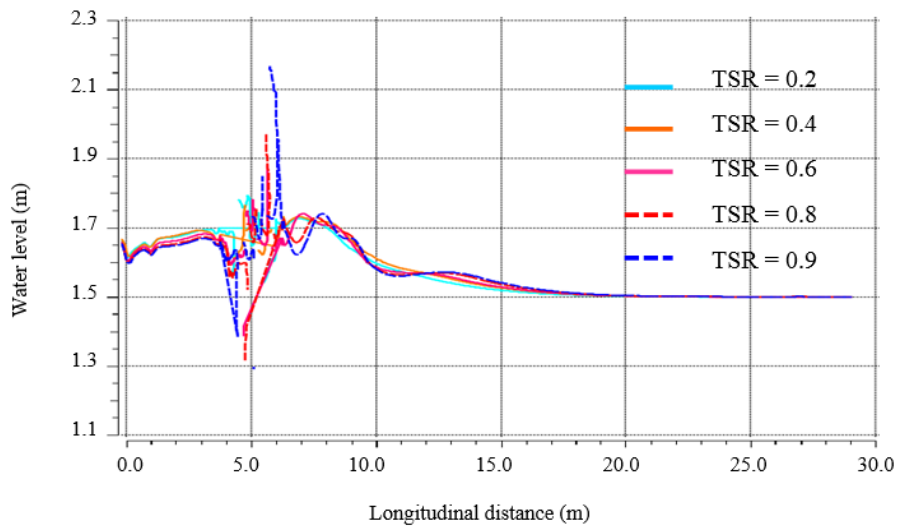


Figure 6. Water level at different distances along the channel at a flow velocity of  $2.0 \text{ m s}^{-1}$

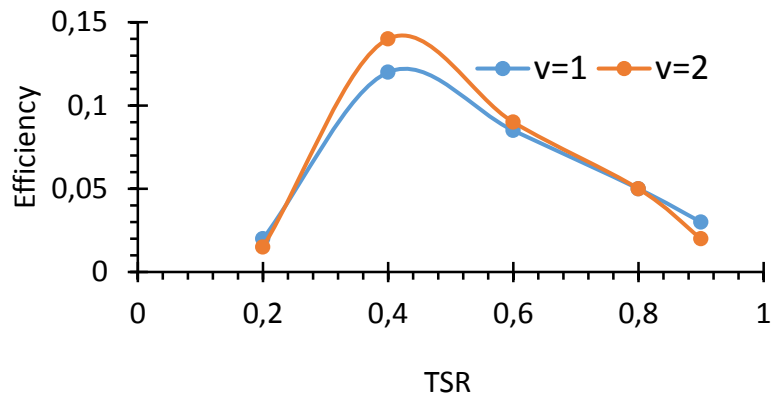


Figure 7. The turbine efficiency at different tip speed ratios

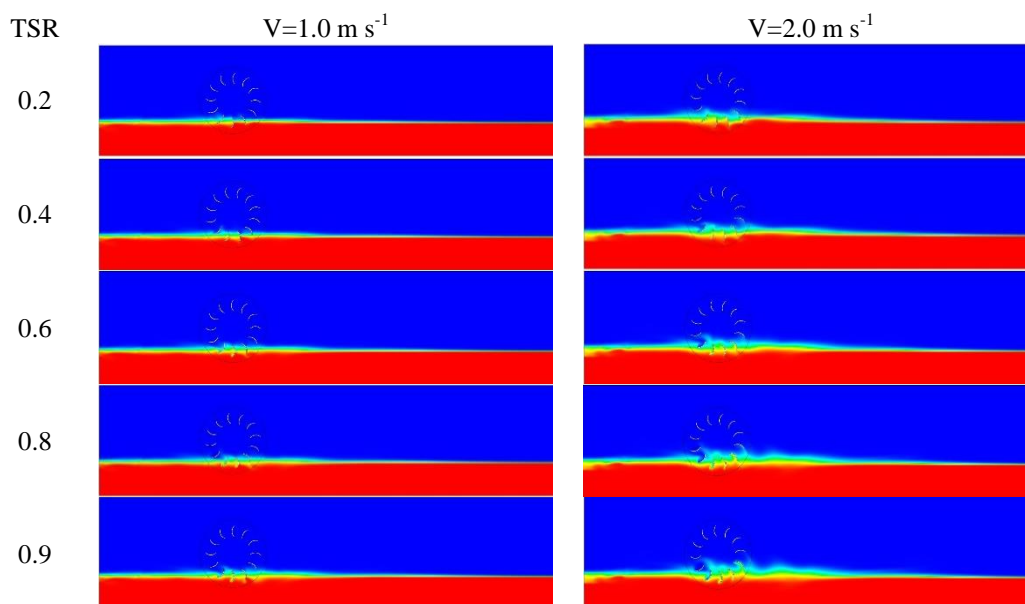


Figure 8. Water volume fraction under different flow conditions and TSRs'

## Conclusions

In the present study, the performance of stream water wheel turbines is evaluated under different flow conditions. Computational fluid dynamics simulations analyses are conducted in order to investigate the suitable streamwise distance between the turbines. The simulation results have shown that in case of constructing a farm of stream water wheel turbines, the distance between the turbines should not be less than 3 times the diameter of the wheel. The flowing water behaved similarly at the two given velocities with high turbulence intensity for the maximum given velocity.

## References

- Biscarini, C., Francesco, S. D. & Manciola, P. (2010). CFD modelling approach for dam break flow studies. *Hydrol. Earth Syst. Sci.*, Vol. 14, pp. 705–718.
- Chevallet, G., Jellouli, M. & Deroo, L. (2012). Democratization of 3D CFD hydraulic models: several Examples performed with ANSYS CFX. *SimHydro: New trends in simulation*. Sophia Antipolis.
- Denny M. The efficiency of overshoot and undershot water wheels. *European Journal of Physics*; 2004. 25: 193-202.
- Institute of Technology – Baghdad – Iraq, 2013.
- Muller G, Denchfield S, Marth R and Shelmerdine R. Stream wheels for applications in shallow and deep water. *Proceedings of 32nd IAHR Congress, Venice, Italy, Theme C2c, paper 291*; 2007.
- Muller G, Kauppert C. Performance characteristics of water wheels. *Journal of Hydraulic Research*; 2004a. 42(5):451-60.
- Paudel S, Linton N, Zanke UCE, Saenger N. Experimental investigation on the effect of channel width on flexible rubber blade water wheel performance, *Renewable Energy*; 2013. 52:1-7.
- Quaschnig V. *Renewable energy and climate change*. Singapore: Wiley; 2010.
- Schlager N, Weisblatt J, editors. *Alternative energy*. Vol.1.China: Thomson Gale; 2006.
- Speziale, C. G., Sarkar, S., & Gatski, T. B. (1991). Modeling the Pressure-Strain Correlation of Turbulence: An Invariant Dynamical Systems Approach. *J. of Fluid Mechanics*, Vol. 227, pp. 245-272.
- Woods G, Tickle A, Chandler P, Beardmore J, Pymm R. Peak power: Developing micro hydropower in the peak district, friends of the peak district, UK; 2010. Available at: <http://www.friendsofthepeak.org.uk/download/files/HYDRO/PEAKPOWERMainreportAppA.pdf>; 2010 [accessed: 30.09.12].

---

### **Author Information**

---

**Mohammad A. Al-Dabbagh**

Northern Technical University, Technical Institute/ Mosul,

Department of water resources techniques

Mosul/ Iraq

Contact e-mail: mohamed.akram@ntu.edu.iq

---